Advancements in molecular medicine

Philips Ingenuity TF PET/MR attenuation correction

Z. Hu,[1] S. Renisch,[2] B. Schweizer,[3] T. Blaffert,[2] N. Ojha,[1] T. Guo,[1]
J. Tang,[1] C. Tung,[1] J. Kaste,[1] V. Schulz,[3] I. Torres,[4] and L. Shao[1]

Abstract

Philips has introduced its first whole body sequential PET/MR system, the Ingenuity TF PET/MR. We present the current status of MR-based attenuation correction (MRAC) technique. MRAC consists of MR image acquisition, segmentation, truncation compensation (TC), μ-value assignment, as well as correction for patient table and RF coils. These components have been described last year; this paper focuses on updates of the two most critical steps of MRAC: segmentation and TC. The segmentation algorithm attempts to distinguish three biological classes: air, lungs, and soft tissue. It combines an intensity-based region-growing technique with lung-model adaptation. For TC, the following three-step approach to correct for truncation in the MR-based attenuation map has been developed and investigated. (A) Areas in the attenuation map which are possibly truncated are identified. (B) For these areas, an estimate of the outer patient contour is extracted from a registered PET image which is reconstructed without attenuation correction. (C) Truncation correction areas as extracted from the PET contours are added to attenuation map. The segmentation algorithm was applied to a number of datasets from a large pool of volunteers from multiple MR systems. The algorithm yields expected results except for susceptibility and motion artifacts. While the truncation compensation algorithm works for most cases, the robustness needs to be further improved.

[1] Nuclear Medicine, Philips Medical Systems, Highland Heights, OH, USA
[2] Digital Imaging, Philips Research, Hamburg, Germany
[3] Molecular Imaging Systems, Philips Research, Aachen, Germany
[4] RWTH, Aachen University, Aachen, Germany

PHILIPS
sense and simplicity

Introduction

Philips has introduced its first whole body sequential PET/MR system. We present the current status of MR-based attenuation correction (MRAC) technique and its validation using data from both PET/MR and PET/CT systems.

MRAC consists of MR image acquisition, segmentation, truncation compensation (TC), and μ-value assignment, as well as correction for patient table and RF coils. These components have been described earlier,[1] but this paper focuses on updates of the two most critical steps of MRAC: segmentation and TC.

Material and methods

MR image segmentation

MR image intensity is generally related to proton density which has no direct correlation with photon attenuation in PET. Thus, the simple approach of PET/CT to scale the CT values to a different energy range in order to construct the attenuation map is not feasible for PET/MR. Our approach employs segmentation of the MR image with subsequent assignment of attenuation coefficients to individual segments. The segmentation algorithm attempts to distinguish three biological classes: air, lungs, and soft tissue.

For whole-body oncology PET/MR applications, special care must be taken to segment the lungs as accurately as possible, since structures that are either missed or incorrectly segmented lead to over- or under-correction in the resulting PET image. In addition, in many patients considerable amount of air is found in the stomach and bowel. This, together with artifacts stemming from the cardiac and respiratory motion, can potentially lead to a poor delineation of the lungs in particular at the diaphragm (see Figure 1).

When using intensity-based methods without regularization based on a prior shape information, this easily leads to "leakage" of lung segmentation into the stomach and bowel. As an example, the center image in Figure 1 shows segmentation results employing region-growing with an intensity threshold as termination criterion. If the intensity threshold is lowered, the leakage improves, but more noise inside the lung also gets segmented, which leads to overcorrection in the PET image.

In order to circumvent these problems, we decided to use a Deformable Shape Model[2] to regularize the segmentation. The model that we used was generated from manual segmentation of more than 20 high-resolution CT datasets. It is a triangle mesh consisting of 3000 triangles, which is sufficient for the current purpose given the limited resolution of MR images.

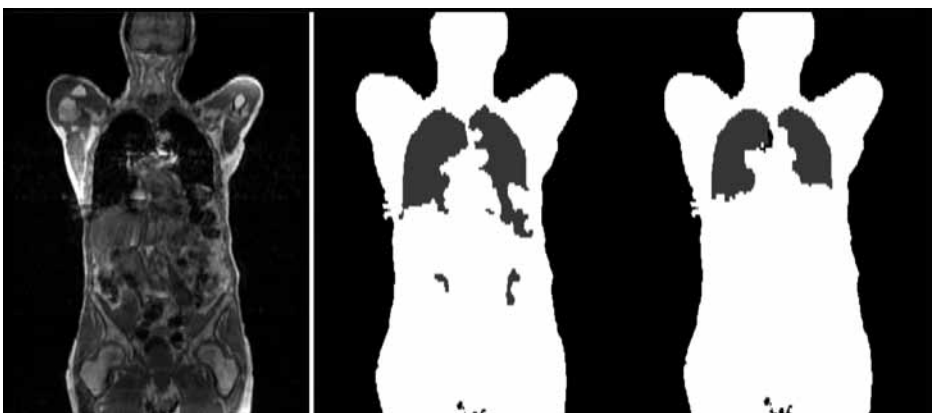

Figure 1 MR image (left), original segmented MR image (middle), and improved segmentation with lung model (right).

The segmentation procedure consists of the following steps. First, the model is initialized using intensity-based lung segmentation with a very low threshold. Then, the model is adapted to the patient image using an energy minimization scheme that minimizes the total energy,

$$E = E_{ext} + \alpha E_{int},$$

consisting of an external energy stemming from the image and an internal energy reflecting the deviation of the mesh from its original shape. During the adaptation, iteratively for every triangle center a new position is determined according to

$$\tilde{\boldsymbol{x}}_i = \boldsymbol{x}_i + d\boldsymbol{n} \operatorname*{argmax}_{j=-l\ldots l}\{\mathrm{F}(\boldsymbol{x}_i + jd\boldsymbol{n}) - Dj^2d^2\}$$

where $\boldsymbol{x}$ is the original position of the triangle center, $\boldsymbol{n}$ is the triangle normal, d is a step size, $k = 2l + 1$ is the number of steps to search, D is a distance weighting factor, and $\mathbf{F}$ is a feature function. In our case we use a step function as feature function (i.e., we expect a profile across the lung wall to look step-like), and we search 30 steps in every direction with 1 mm distance with $D = 0.5$. The internal energy restricts the movement of the mesh vertices. A more detailed explanation is provided here.[2] The external energy is then computed as

$$E_{ext} = \sum_i w_i \left(\frac{\boldsymbol{g}(\boldsymbol{x}_i)}{\|\boldsymbol{g}(\boldsymbol{x}_i)\|}(\tilde{\boldsymbol{x}}_i - \boldsymbol{x}_i)\right)^2,\ w_i = \max\{\mathrm{F}(\boldsymbol{x}_i + jd\boldsymbol{n}), 0\}$$

with $\boldsymbol{g}(\boldsymbol{x}_i)$ being the image gradient at position $\boldsymbol{x}_i$.

The internal energy restricts the movement of the mesh vertices and is defined as

$$E_{ext} = \sum_i \sum_{k \in Neighbors(i)} (\boldsymbol{v}_i - \boldsymbol{v}_k - s\boldsymbol{R}(\boldsymbol{v}_{i0} - \boldsymbol{v}_{k0}))^2$$

with $\boldsymbol{v}_i$ and $\boldsymbol{v}_k$ being the new vertex positions, $\boldsymbol{v}_{i0}$ and $\boldsymbol{v}_{k0}$ being the original vertex positions, s is a scaling factor and $\boldsymbol{R}$ is a rotation matrix; for a more detailed explanation see [model]. In our case we use an external energy weight of $a = 0.2$.

Applying this iteration scheme, the mesh model is adapted to the individual patient dataset. Since it is well known that such mesh adaptation schemes are difficult to adapt to pointed edges (like the lower lung edges), some post-processing needs to be applied. We use a region-growing technique with two constraints, one being an intensity threshold that is estimated from the intensity distribution and the other being a distance criterion, i.e., the segmented voxel shall be inside the mesh model or not further than 2 cm outside of it. This constraint is efficiently applied via a distance map. In order to get rid of remaining noise voxels, morphological opening with a 6-star kernel of 1 voxel size is applied in addition. This scheme led in most clinical cases to acceptable lung segmentation.

MR image truncation compensation

The usable MRI FOV tends to be lower than the bore size, which causes MR image truncation close to FOV edge. This effect is most obvious in large patients or with patients holding their arms down during acquisition. While this image truncation may not normally be relevant in diagnostic MR evaluation, it leads to truncated and thus unrealistic attenuation maps for the PET reconstruction.

The following three-step approach to correct for truncation in the MR-based attenuation maps for PET has been developed and investigated. (A) Areas in the attenuation map which are possibly truncated are identified. (B) For these areas, an estimate of the outer patient contour is extracted from a registered PET image which is reconstructed without attenuation correction. (C) Truncation correction areas as extracted from the PET contours are added to attenuation map.

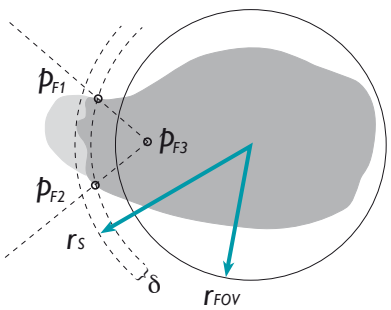

Figure 2 Schematic illustration of edge detection approach for truncated areas in MR.

In step (A), the uncorrected attenuation map is tested slice-by-slice for sections extending beyond a safe inner disk with a radius of slightly less than the known FOV of r_{FOV} = 230 mm. Each such section is considered as being potentially truncated. In Figure 2, a patient axial slice is illustrated, with the dark grey area visible in the MR image, while the light grey area has been truncated. For each section outside of the FOV, the tissue point lying farthest out with respect to the center of the MR FOV is detected and its radial distance r_S to the center is calculated. Two feature points p_{F1} and p_{F2} are extracted by determining the intersections of each section with a circle of radius r_S-δ, with δ being an empirical value describing the typical size of the MR image's rim distortion due to truncation. A central point p_{F3} is added on the normal line passing the middle of the connection between the two feature points. The lines from p_{F3} to the other two feature points span a fan in which the contour search of the step (B) is being performed. This approach provides on the one hand that truncation areas are properly detected, on the other hand it conserves as much as possible from the existing MR information.

In step (B), the corresponding fan area in a registered, non-attenuation-corrected PET image is used to detect an outer patient contour. This is performed by applying a multi-scale approach and a canny edge search on the PET data. The outmost contour information of the two algorithms is used to derive the boundary information. The area enclosed by the connection line between p_{F1} and p_{F2} and the newly detected contour line is filled with attenuation values corresponding to soft tissue and is inserted in step (C) into the slice in the attenuation map.

Here, optional morphological filtering can be performed on the entire volume of truncation compensations in order to smooth it mainly in z-direction. A compensation example is shown in Figure 3, where the truncated areas are filled with the attenuation value of soft tissue.

The non-attenuation corrected PET (NAC) image is a good candidate for deriving the body contour to achieve the goal of MR image truncation compensation in the context of MR-based PET attenuation correction. Its main advantage is that it is almost readily available, as neither correction nor fine sampling of the raw data is required for the reconstruction. It is to be noted, however, that this image does often exhibit excessive image intensity distribution that prevents one from deriving a well-defined body contour. A class of artifacts related to the image characteristics of the NAC image is the concave-structure problem, as shown in Figure 4. The shape of concave structures in the truncated area (e.g., armpits and areas around the female breast) can't be reproduced correctly by the truncation compensation algorithm. The cause for this is that the corresponding NAC image typically only contains an outer body contour which corresponds to the convex hull of the activity-filled areas.

An alternative approach is to use the NAC image reconstructed with Time-of-Flight information (TOF-NAC), as shown in Figure 4. The TOF-NAC image clearly shows better boundary definition than the NAC image and thus represents a more promising perspective.

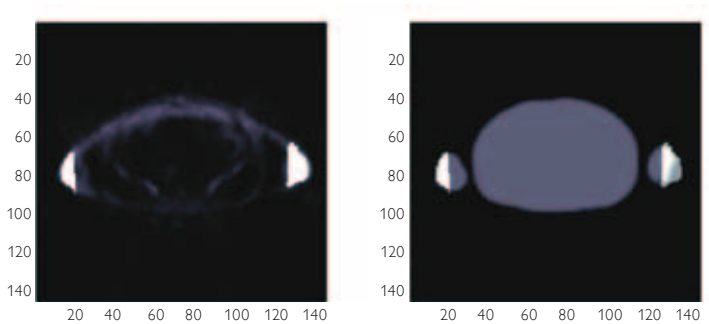

Figure 3 Slice of attenuation map with effect of TC overlaid as bright areas (right). Corresponding slice of the non-attenuation corrected PET image (left).

Results and discussion

MR image segmentation

The segmentation algorithm was applied to a number of datasets (n>100) from a large pool of volunteers from multiple MR systems. The algorithm yields expected results except for susceptibility and motion artifacts. Application of respiratory gating could potentially mitigate respiratory motion artifacts. The MR image artifact introduced by a metal implant (Figure 5) cannot unfortunately be accounted for in the current segmentation algorithm.

MR image truncation compensation

In the earlier publication,[1] a slightly simplified version of this truncation compensation approach has been investigated on simulated truncations. In these studies, artificially truncated attenuation maps were generated out of non-truncated CT data from PET/CT studies. The truncation compensation algorithm was then applied to these maps and its effect was compared to the known body contour from the CT data.

In the current study, we demonstrate the effect of truncation compensation in the real PET/MR image processing pipeline of the novel Philips whole-body PET/MR system. The MR maps acquired for the purpose of attenuation correction are in a first pass converted to attenuation values in a segmentation pipeline. This pipeline was described earlier and performs a separation of the outer region from the patient volume, identifies the lungs by a combined intensity-based and model-based segmentation and features further processing steps to deal with small structures and bowel air. At this point in time, the resulting attenuation map consists basically of three material types: air, soft tissue, and lung tissue. This map represents the input data for the truncation compensation algorithm.

The purpose of this investigation was to demonstrate the fidelity of truncation compensation on PET/MR patient data. Since no ground truth (i.e., a non-truncated patient image) was available, the validation strategy consisted of visual interpretation of the TC images. For this purpose, the non-attenuation-corrected PET image and the uncorrected and corrected attenuation map were analyzed in parallel slice by slice.

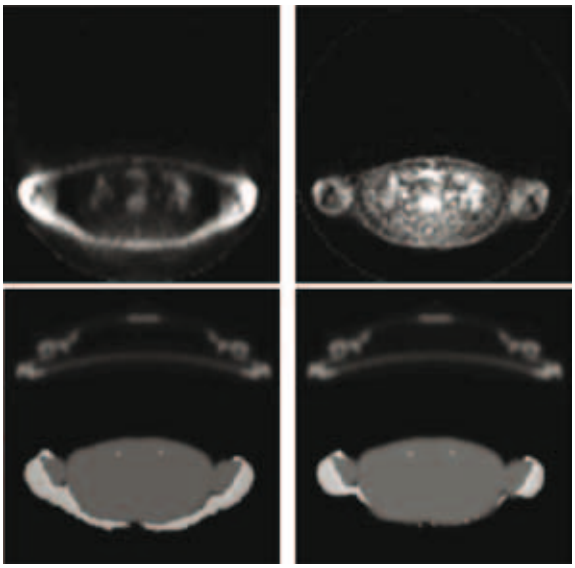

Figure 4 NAC image (top left) and the truncation compensated attenuation map with the NAC image (bottom left), compared with the TOF-NAC image (top right) and the truncation compensated attenuation map with the TOF-NAC image (bottom right).

Figure 5 A big hole in the MR image (left) created by a cardiac stent on the chest gets translated into the attenuation correction map (middle); subsequently the impact on the final reconstructed PET image is visible (left).

The truncation-compensated areas were identified by a direct comparison of the two attenuation maps. The corrections in the attenuation map slices were rated for shape agreement with the PET boundary as well as for rim continuity between the original and the added soft tissue information. A difference of more than two voxels (8 mm) was considered a failure of the algorithm. One example of successful TC is displayed as coronal view in Figure 6. It is, however, not easy to find any apparent differences when directly comparing the two final reconstructed PET images before and after the TC being applied. The difference image does reveal dramatic quantitative changes around the arms region where the truncation compensation has the biggest effect. As far as the main trunk of the body is concerned, the observed difference is within a few percent for inner anatomic structures while relative changes are much higher close to the surfaces of the structures due possibly to lower counting statistics.

A set of 30 patient cases, covering a total of over 5000 axial slices, was investigated. These cases included truncation at the chest and torso in large patients, truncations at the arms in arms-next-to-the-body scanning position, as well as truncation at the arms in arms-up scanning position. The observed percentage statistics for TC is displayed in Figure 7. Overall about 63% of the slices were not truncated and about 27% were successfully compensated for truncation, while for the remaining 10% of the slices TC was suboptimal.

Several challenging scenarios were identified where the current TC algorithm tends to falter:

1. The shape of concave structures in the truncated area (e.g., armpits and areas around the female breast) can't be reproduced correctly by the TC algorithm, as shown in Figure 4.
2. For very large patients even the PET image itself was truncated. This led to improper TC since no realistic patient contour could be extracted from the PET data.
3. Large gaps were present between the arms and the body. These resulted in truncated arm cross sections which appeared as small, isolated spots in transverse plane, as shown in Figure 8.

Improvements to the algorithm to address these specific issues are being currently implemented, in particular by using the Time-of-Flight-based non-attenuation-corrected PET images (TOF-NAC), as shown in Figure 4.

It is also to be noted that the current TC algorithm is targeted primarily for the PET imaging with FDG as radioactive tracer. For the PET applications with other tracers, further investigation is required to determine its applicability.

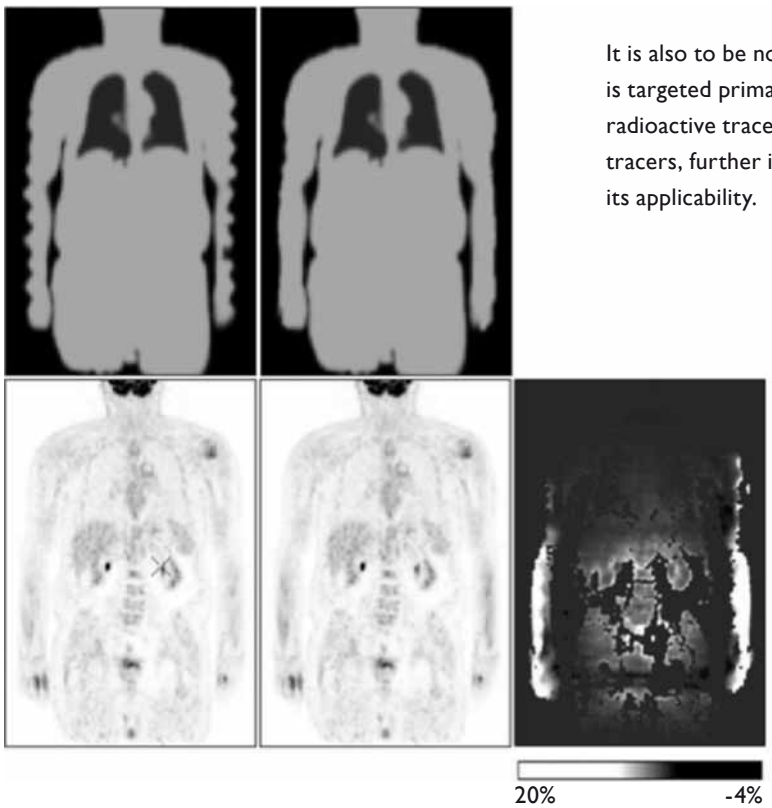

Figure 6 Example of successful truncation compensation.
Left: MR-based attenuation map (top) and reconstructed PET image (bottom) before TC.
Middle: MR-based attenuation map (top) and reconstructed PET image (bottom) after TC.
Right: Relative percentage difference between the PET images with and without truncation compensation.

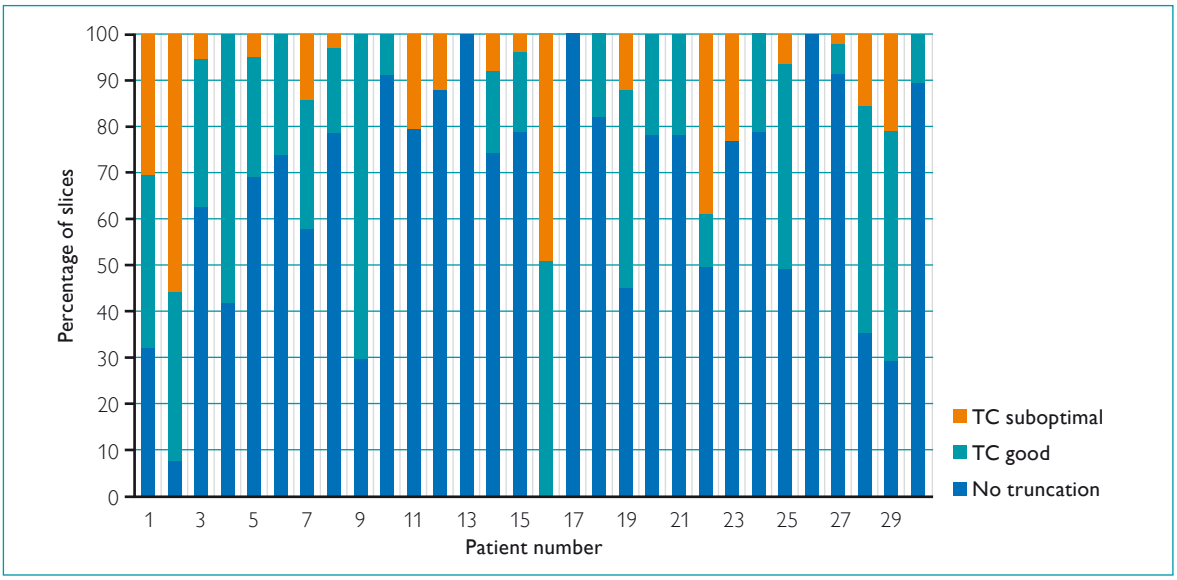

Figure 7 Performance statistics of truncation compensation (TC).

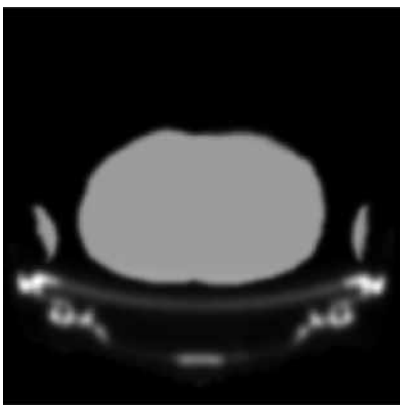

Figure 8 Axial slice of attenuation map where truncated arms appear as small, isolated spots.

Conclusion

We have implemented and improved the MR-based attenuation correction method for a clinical whole-body PET/MR system. While awaiting future clinical validation, the algorithm is promising from preliminary patient data evaluation. Although the 3-segment MRAC resembles the results from short PET transmission scans, future work might be needed to implement and validate segmentation of more tissue classes, such as cortical bone, fat, and muscle.

References

1. Hu Z. et al. MR-based attenuation correction for a whole-body sequential PET/MR system. IEEE NSS/MIC Conf. Rec., Orlando. 2009;3508-3512.
2. Lorenz C. et al. 3D Statistical Shape Models for Medical Image Segmentation. Proc. Int. Conf. on 3D Imaging and Modeling, Ottawa. 1999;0414.

Philips Healthcare is part of Royal Philips Electronics

How to reach us
www.philips.com/healthcare
healthcare@philips.com

Asia
+49 7031 463 2254

Europe, Middle East, Africa
+49 7031 463 2254

Latin America
+55 11 2125 0744

North America
+1 425 487 7000
800 285 5585 (toll free, US only)

Please visit www.philips.com/IngenuityTFPETMR

Printed in The Netherlands.
4522 962 81661 * DEC 2011